https://ntrs.nasa.gov/search.jsp?R=19660010220 2018-07-23T15:31:13+00:00Z

NSG-137

N66-19509
(ACCESSION NUMBER) (THRU)
38 1
(PAGES) (CODE)
CR 71084 23
(NASA CR OR TMX OR AD NUMBER) (CATEGORY)
FACILITY FORM 602

HC. $2.00
MF. .50

POLARIZATION, DIRECTIONAL DISTRIBUTION, AND OFF-SPECULAR PEAK PHENOMENA IN LIGHT REFLECTED FROM ROUGHENED SURFACES

K. E. Torrance and E. M. Sparrow
University of Minnesota, Minneapolis, Minnesota

and

R. C. Birkebak
Georgia Institute of Technology, Atlanta, Georgia

ABSTRACT

19509

The directional distribution of the reflected thermal radiation from surfaces of varying roughness is explored experimentally. Measurements were made of the plane-polarized components of the reflected radiation as well as of the mixed radiation (containing all components of polarization). The test materials included magnesium oxide ceramic and aluminum coated ground glass, thereby permitting a study of reflection in the presence and in the absence of sub-surface scattering. The angle of incidence was varied from 10 to 87°, while the angle of reflection extended from 0 to 89°. The roughness of the test surfaces ranged from optically smooth to 5.8 μ, while the measurements were performed monochromatically at a wavelength of 0.5 μ. The measured directional distributions affirm that the diffuse limit (Lambert's cosine law) does not hold when roughened surfaces are illuminated at moderate to large angles of incidence. Rather, it is found that a maximum in the distribution of the reflected intensity occurs at reflection angles larger than the specular-ray direction. The contributions of the s- and p-components of polarization to this off-specular peak are delineated. The degree of polarization imparted by reflection at surfaces of varying roughness is also investigated. It is shown that the absence or presence of sub-surface scattering is an important factor. The various findings of the experiments are subjected to interpretation by a model of the reflection process which pictures the surface as being composed of elementary mirror-like facets.

author

INTRODUCTION

This paper is concerned with the effects of surface roughness and angle of incidence on the directional distribution and polarization of reflected thermal radiation. There are two limiting cases which are widely regarded as bounds for the directional reflection characteristics of real surfaces, these are diffuse reflection and specular reflection. It has been verified both experimentally and analytically,[1-6] that for any fixed wavelength, specular reflection is approached as the surface roughness decreases. On the other hand, recent experiments[7] have shown that at a fixed wavelength, the diffuse limit is approached with increasing surface roughness only when the angle of incidence is near-normal. At moderate and large angles of incidence, the diffuse limit is not approached as the surface roughness increases. Instead, one finds a maximum in the distribution of the reflected intensity at a reflection angle (relative to the normal) larger than the specular angle.

One of the aims of this research is to provide new information on the aforementioned off-specular maxima which contributes to their understanding. Specific consideration is given to the contributions of the separate components of polarization to the directional distributions and to the off-specular maxima. The experiments were performed using a metal and a nonmetal which had widely different

---

[1] A. F. Gorton, Physical Review, vol. 7, 1916, p. 66.

[2] H. Davies, Proceedings of the Institution of Electrical Engineers, vol. 101, 1954, p. 209.

[3] H. E. Bennett and J. O. Porteus, Journal of the Optical Society of America, vol. 51, 1961, p. 123.

[4] H. E. Bennett, Journal of the Optical Society of America, vol. 53, 1963, p. 1389.

[5] R. C. Birkebak and E. R. G. Eckert, Journal of Heat Transfer, Trans. ASME, Series C, vol. 87, 1965, p. 85.

[6] K. E. Torrance and E. M. Sparrow, Journal of Heat Transfer, Trans. ASME, Series C, vol. 87, 1965, p. 283.

[7] K. E. Torrance and E. M. Sparrow, American Society of Mechanical Engineers Paper 65-WA/HT-19, to be published in the Journal of Heat Transfer, Trans. ASME, Series C.

polarization characteristics. For each material, test surfaces of various roughnesses were prepared and investigated.

The extent of the polarization imparted by the reflection of unpolarized incident radiation from a given material depends on the surface condition, the angle of incidence, and the wavelength. For optically smooth surfaces, the degree of polarization at any angle of reflection is fully specified by the Fresnel equations. The effect of surface roughness and angle of incidence on the degree of polarization is explored experimentally as part of this investigation.

In performing the experiments, the test surfaces were illuminated by a narrow beam of radiation inclined at a pre-selected angle relative to the surface normal. The reflected radiation was collected in a pre-selected angular direction in the plane of incidence, whereupon it was passed through a polarizer and then into a spectrometer for wavelength resolution. The angle of incidence ranged from 10 to 87°, while the angle of reflection was varied from 0 to 89°. All reflection measurements were performed at a wavelength $\lambda = 0.5\,\mu$. The test surfaces were either of magnesium oxide ceramic, a weakly-absorbing, internally-scattering dielectric, or of evaporated aluminum on a glass substrate. A total of nine test surfaces were employed, ranging in roughness from a high polish to a root-mean-square value of $5.8\,\mu$. Further details of the experimental method will be described after appropriate background literature is discussed.

The existence of off-specular maxima was observed as early as 1903 by Thaler.[8] Such peaks have been inherent in the reflection data of many investigators since that time, but in the majority of cases the phenomenon went undetected or was not discussed. A survey of pertinent contributions to the subject is presented elsewhere.[7] A physical model purporting to explain the off-specular maxima was first proposed by Pokrowski.[9] The Pokrowski model, in common with

[8] F. Thaler, Annalen der Physik, vol. 11, 1903, p. 996.

[9] G. I. Pokrowski, Zeitschrift für Physik, vol. 30, 1924, p. 66; vol. 35, 1925, p. 34; vol. 36, 1926, p. 472.

most subsequent ones, postulated specular reflection obeying Fresnel's equations from small mirror-like facets on the surface, plus a diffuse scattering that originates either on the surface or internal to the material. Pokrowski attributed his measured off-specular peaks to reflection from the facets. Later, Schulz[10] modified the Pokrowski model by giving a statistical distribution of slopes to the mirror-like facets on the surface.

More recently, Middleton and Mungall[11] observed off-specular peaks in the angular distribution of light reflected from snow and ice surfaces. To explain the experimental findings, an analytical model of the reflection process was proposed. This model was similar to that of Pokrowski-Schulz, but included a multiplicative factor to account for the incomplete illumination of the mirror-like facets due to shadowing by adjacent facets. Thus formulated, the model predicts certain trends characteristic of the experimental data of Middleton and Mungall.

Within the knowledge of the present authors, there have been no prior measurements of angular distributions of the plane-polarized reflection components, nor have there been attempts to relate such information to the off-specular peaks.

Experimental information on the state of polarization of radiation reflected from rough surfaces would be of general value in fostering an understanding of the reflection process at such surfaces. However, to be useful in this connection, the measurements would have to extend over a wide range of incidence and reflection angles. Much of the literature on polarization by reflection does not meet this requirement.[12-16] The recent work of Gorodinskii,[17] however, covered such an

[10] H. Schulz, Zeitschrift für Physik, vol. 31, 1925, p. 496.

[11] W.E.K. Middleton and A. G. Mungall, Journal of the Optical Society of America, vol. 42, 1952, p. 572.

[12] N. A. Umow, Physikalische Zeitschrift, vol. 6, 1905, p. 674.

[13] D. Chmyrow and N. Slatowratsky, Physikalische Zeitschrift, vol. 7, 1906, p. 533.

[14] V. Návrat, Sitzungsberichte der Akademie der Wissenschaften in Wien (Vienna), mathematisch-naturwissenschaftlichen Klasse, vol. 120, 2a, 1911, p. 1229.

[15] M. Leontowitsch, Zeitschrift für Physik, vol. 46, 1927, p. 739.

[16] W. A. Rense, Journal of the Optical Society of America, vol. 40, 1950, p. 55.

[17] G. M. Gorodinskii, Optics and Spectroscopy (translation of Optika i Spectroskopiya by the Optical Society of America), vol. 16, 1964, p. 59.

angular range.

Gorodinskii studied the degree of polarization of visible light after reflection from roughened samples of dark glass, but did not measure angular distributions. Such a glass reduces the effect of internal scattering, with a resulting dominance of the role of surface reflection. Curves portraying the degree of polarization of light reflected in the specular direction were presented for a range of incidence angles. These results demonstrate that as the surface roughness decreases, the Fresnel limit is approached. Furthermore, for each of three angles of incidence, Gorodinskii shows the dependence of the degree of polarization on the angle of reflection in the incident plane. For each incident angle, the curves for the various surface roughnesses peak at approximately the same reflection angle. The angular position corresponding to the peak is shown to be related to the polarizing angle[18] of radiation incident upon and specularly reflected from the mirror-like facets of the roughened surface. Indeed, it is found that the sum of the aforementioned reflection angle plus the angle of incidence is equal to twice the polarizing angle. Thus, the measurements of Gorodinskii shed some light on the mechanism of reflection from a highly-absorbing dielectric.

The investigation of Gorodinskii and the findings resulting therefrom correspond to a specific type of material. It is of interest to investigate different types of materials with a view to discerning in what ways (and why) the degree of polarization is altered.

EXPERIMENTAL APPARATUS

A schematic diagram of the experimental apparatus is shown in Fig. 1 and a photograph is presented in Fig. 2. The flow path of the radiation can be described with the aid of Fig. 1. The output of a radiation source A is focused by mirror B onto the test surface C (normal $\hat{N}$). Radiation reflected from the

[18] The polarizing (Brewster) angle is that angle at which the parallel-polarized component (parallel to the plane of incidence) reflected from a smooth surface is a minimum.

test surface in a pre-selected direction is collected by mirror D and brought to a focus on the entrance slit of the spectrometer F. The resulting monochromatic output from the spectrometer is sensed by a detector located at G. A polarizer E is inserted into the beam to facilitate measurements of the degree of polarization.

The optical system external to the spectrometer includes a multiple-yoke device by which the directions of the incident and reflected beams can be varied independently and with precision. Figure 2 shows a complete view of the entire test apparatus looking toward the spectrometer and the multiple-yoke, which, respectively, appear at the left and at the right. The multiple-yoke apparatus is capable of orienting the sample so that radiation reflected into any angular direction in the hemispherical space above the test surface can be measured for any angle of incidence.[6] In Fig. 2, the device is shown in position for a measurement out of the plane of incidence.[19]

The measurements reported here, however, were confined to the plane of incidence. Consequently, the angular orientations of the incident and the reflected beams can each be characterized by a single coordinate angle, as shown in Fig. 1 The incident direction is specified by the polar angle Ψ, measured with respect to the surface normal. The direction of reflection is characterized by the polar angle θ, also measured from the surface normal.

In order to vary the polar angles Ψ and θ, two turntables are used. In Fig. 1, the axes of these turntables are coaxial, lying perpendicular to the plane of the schematic diagram and in the plane of the sample surface. The radiant energy focused by mirror B onto the sample surface is centered on the turntable axes. The larger of the two turntables supports the source A, mirror B, and sample C. It thus permits rotation of these components as a unit in order to vary the reflection angle θ. The smaller turntable rotates only the sample in

[19] The plane of incidence includes the incident beam and the surface normal.

order to vary the incidence angle Ψ. The angular settings of the two turntables are read from graduated circles with vernier indicators.

Pertinent details of the optical system are as follows: The radiation source[20] employed for measurements in the visible region is a 5/8-in. diameter fluorescent bulb masked to 1/2 by 3/4 in. Mirror B is a spherical mirror with an aluminum first surface (d = 1 in., f = 8 in.); it subtends a solid angle of $\pi/1024$ steradians with respect to both the source and the test specimen. The area of the specimen that is illuminated under normal incidence is 1/2 in. by 3/4 in. The 1/2 in. dimension is increased by the factor $(\cos \Psi)^{-1}$ for other angles of incidence Ψ. The collecting mirror D is also a spherical mirror with an aluminum first surface (d = 2 in., f = 16 in.); it subtends a solid angle of $\pi/1024$ steradians with respect to both the test sample and the entrance slit of the spectrometer. The entrance slit has a maximum width of 0.084 in. and is masked to a height of 5/16 in. The slit width was adjusted so that the radiant energy focused onto it by mirror D always filled the slit completely. The commercial sheet polarizer E is mounted so that the plane of polarization can be rotated through 90° (E is not shown in Fig. 2).

The aforementioned fluorescent source emits radiation consisting of a continuous emission spectrum peaking at $\lambda = 0.5\mu$ with a superimposed line spectrum. The measurements presented here were performed at $\lambda = 0.5\mu$, a region quite far removed spectrally from the aforementioned emission lines. The spectrometer is a Perkin-Elmer model 112-U from which the standard source assembly had been removed. A fused-quartz prism and photomultiplier-tube detector were used for resolving and sensing the radiant energy, respectively.

TEST SPECIMENS AND THEIR PREPARATION

The two materials employed in this investigation were selected on the basis

[20] An alternative infrared source consisting of a globar enclosed in a water-cooled jacket is available and is shown in Fig. 2.

of their reflection properties. The fused polycrystalline magnesium oxide ceramic is a white dielectric material characterized by weak absorption and strong internal scattering of visible light. Thus, both surface and internal reflection contribute. This is in contrast to the dark-colored dielectric studied by Gorodinskii.[17] Such a dark material strongly absorbs light which is transmitted through the surface, minimizing the role of internally-reflected radiation and accentuating surface reflection. The second material employed here, evaporated aluminum on ground glass, is similar to that of Gorodinskii's dielectric in that reflection occurs essentially at the surface, but possesses metallic reflection characteristics.

The fused polycrystalline magnesium oxide is of high purity (99.9 percent) and was supplied by Honeywell Incorporated. It is the same material employed in reference 6. The four test specimens had surface dimensions 3/4 in. by 1/2 in. and were 1/4 in. thick. The specimens were mounted in standard lucite metallurgical sample holders; a typical specimen is shown in place on the apparatus in Fig. 2. Auxiliary transmission measurements at $\lambda = 0.5\mu$ showed that the 1/4 in. thickness of the sample was sufficient to preclude effects of the specimen holder.[21]

Five ground glass discs 1 1/4 in. in diameter and 1/4 in. thick were employed as substrates for the second group of test surfaces. These were simultaneously coated with evaporated aluminum of high purity while under vacuum.

All test surfaces were initially polished flat using a standard optical polishing technique. Subsequently, a similar technique was used to roughen eight of the nine specimens with the grinding grits as listed in Table 1.

The surface roughness of the test specimens was measured with a high-precision stylus profilometer, the Taylor-Hobson Talysurf Model 3. The tip of the sensor was a diamond stylus of 1.25μ (0.00005 in.) radius. A standard roughness-width cutoff length of 0.030 in. was used in determining the root-mean-square mechanical

[21] K. E. Torrance, Thesis in the Mechanical Engineering Department, University of Minnesota, Minneapolis, Minnesota, January, 1964.

roughness values σ_m listed in Table 1. The roughness measurements for the aluminum coated ground glass were made after the coating had been applied.

EXPERIMENTAL EVALUATION OF THE BIANGULAR REFLECTANCE

Definition of the reflectance. The angular distribution and the degree of polarization of reflected radiation were evaluated in terms of the biangular reflectance. The designation biangular stems from the fact that two angular specifications are involved: The angle of illumination and the angle of reflection. The definition of the biangular reflectance used in this study is in accord with that of other investigators.[22-24]

The biangular reflectance of the mixed radiation (containing all polarization components) is denoted here by the symbol ρ. It is defined as the reflected intensity dI_r in the direction θ divided by the radiant energy de_i incident per unit time and unit area on the surface and contained in a solid angle $d\omega_i$ inclined in the direction ψ relative to the surface normal, that is

$$\rho(\psi,\theta)=\frac{dI_r(\psi,\theta)}{de_i(\psi)} \tag{1}$$

When a pair of angles appears within parentheses, the first angle corresponds to the direction of the incident beam and the second angle corresponds to the direction of the reflected beam. A single angle in parentheses is used for quantities which have only one angular dependence.

The intensity of radiation is defined as follows: First, let de denote the radiant energy per unit time and unit area contained within an infinitesimal solid angle $d\omega$ that is inclined at an angle β relative to the surface normal. Then, the intensity is given by the ratio of de to the product $\cos\beta\ d\omega$. In

[22] H. J. McNicholas, Journal of Research of the National Bureau of Standards, vol. 1, 1928, p. 29.

[23] C. von Fragstein, Optik, vol. 12, 1955, p. 60.

[24] Theory and Fundamental Research in Heat Transfer, edited by J. A. Clark, Pergamon Press, New York, N.Y., 1963, p. 7.

accordance with this definition, the intensity of the incident radiation is written as

$$I_i(\Psi) = \frac{de_i(\Psi)}{\cos\Psi \, d\omega_i} \tag{2a}$$

The intensity of the radiation reflected from a scattering surface is realistically a small quantity and is correspondingly expressed as

$$dI_r(\Psi,\Theta) = \frac{d^2 e_r(\Psi,\Theta)}{\cos\Theta \, d\omega_r} \tag{2b}$$

The plane-polarized biangular reflectances are respectively denoted by ρ_s and ρ_p. The subscript s is used to distinguish the component polarized perpendicular to the plane of incidence, the letter s stemming from the German word for perpendicular, "senkrecht." The subscript p distinguishes the component polarized parallel to the plane of incidence.

The biangular reflectances for the plane-polarized components are defined in a manner analogous to that for the mixed radiation, that is

$$\rho_s(\Psi,\Theta) = \frac{dI_{r,s}(\Psi,\Theta)}{de_i(\Psi)/2} \quad , \quad \rho_p(\Psi,\Theta) = \frac{dI_{r,p}(\Psi,\Theta)}{de_i(\Psi)/2} \tag{3}$$

The quantities $dI_{r,s}$ and $dI_{r,p}$ are the reflected intensities of the perpendicular and parallel-polarized components. Furthermore, since the incident beam is unpolarized, the incident radiant flux carried by each component is $de_i/2$. Inasmuch as $dI_r = dI_{r,s} + dI_{r,p}$, it follows from equations (1) and (3) that

$$\rho(\Psi,\Theta) = \frac{1}{2}\left[\rho_s(\Psi,\Theta) + \rho_p(\Psi,\Theta)\right] \tag{4}$$

By using the reflectances defined in equations (3), the degree of polarization of a reflected beam can be stated as

$$\text{Degree of Polarization} = \frac{\rho_s - \rho_p}{\rho_s + \rho_p} \tag{5}$$

Inasmuch as ρ_s and ρ_p depend on the angles Ψ and Θ, so also does the degree of polarization.

In the present application of the foregoing definitions, the solid angle $d\omega_i$, subtended by the incident beam, is equal to the solid angle $d\omega_r$ of the reflected beam. Furthermore, all expressions are applied monochromatically.

Experimental evaluation of reflectances. The reflectance measurements performed during this investigation are of three types. First, the angular distributions of the plane-polarized and the mixed biangular reflectances were measured relative to the mixed biangular reflectance in the specular direction. These measurements were carried out for a range of incidence angles. Second, the degree of polarization was determined over a broad range of incidence and reflection angles. Third, in order to provide information on the absolute value of the reflectance, the mixed biangular reflectance in the direction of the surface normal was determined as a function of the angle of incidence. This biangular reflectance is termed the mixed normal biangular reflectance.

The experimental determination of the biangular reflectance is greatly facilitated because the spectrometer output is directly proportional to the intensity of the reflected radiant beam. This proportionality stems from the fact that both the solid angle $d\omega_r$ and the projected area of the test specimen, as viewed by the spectrometer, are not altered as the angle of reflectance is varied. The constancy of the projected area occurs because the spectrometer entrance slit, which is always fully illuminated, has a smaller area than the illuminated spot on the specimen.

In performing the measurements, proper account must be taken of the background radiation. This consists of emission from the sample, the optics, and the surroundings. The level of the background radiation in the visible region of the spectrum was minimized by performing the experiments in a darkened room. The background level was determined for each angular orientation of interest by shuttering mirror B (Fig. 1). Therefore, the absolute intensity of radiation

reflected from the test sample in the direction θ, denoted by $\Delta I_r(\psi,\theta)$, is proportional to the detector output minus the corresponding background value. The Δ-symbol is used in place of the differential d to indicate a finite, experimentally-determined quantity.

For a given test specimen, the ratio of the mixed biangular reflectance in an arbitrary direction θ to the mixed biangular reflectance in the specular direction is evaluated from equation (1) in terms of measured quantities as

$$\frac{\rho(\psi,\theta)}{\rho(\psi,\psi)} = \frac{\Delta I_r(\psi,\theta)}{\Delta I_r(\psi,\psi)} \tag{6a}$$

for a given angle of incidence ψ. The plane-polarized biangular reflectances relative to the mixed biangular reflectance in the specular direction are similarly evaluated from equations (1) and (3) as

$$\frac{\rho_s(\psi,\theta)}{\rho(\psi,\psi)} = 2\cdot\frac{\Delta I_{rs}(\psi,\theta)}{\Delta I_r(\psi,\psi)} \quad , \quad \frac{\rho_p(\psi,\theta)}{\rho(\psi,\psi)} = 2\cdot\frac{\Delta I_{rp}(\psi,\theta)}{\Delta I_r(\psi,\psi)} \tag{6b}$$

In any prism-type spectrometer, there is a polarizing effect owing to differential reflection of the two components of polarization at the prism faces. The extent of the polarization due to the spectrometer was determined from auxiliary experiments, and an appropriate correction was applied in evaluating equations (6b) However, as will be discussed later, the correction was not applied to equation (6a) in order to facilitate a display of the extent of the spectrometer polarization.

The degree of polarization was evaluated by introducing the corrected plane-polarized biangular reflectances into equation (5). Alternatively, the degree of polarization could be determined by simply measuring the relative intensities of the s- and p-compoents and correcting for spectrometer polarization. Thus,

$$\text{Degree of Polarization} = \frac{1 - \rho_s/\rho_p}{1 + \rho_s/\rho_p} \tag{7}$$

Equation (7) was applied in those cases in which the angular distribution of reflected radiation was not measured.

The mixed normal biangular reflectance corresponding to various incidence angles was conveniently measured relative to a reference value of the normal biangular reflectance. The absolute magnitude of the latter quantity was determined from an independent experiment.

ANGULAR DISTRIBUTIONS OF MIXED AND PLANE-POLARIZED REFLECTANCES

The experimentally-determined angular distributions of the mixed and plane-polarized biangular reflectances are presented in Figs. 3 to 7. Among these, Figs. 3 to 6 contain results for magnesium oxide ceramic, while Fig. 7 pertains to aluminum coated ground glass. In all figures, the biangular reflectances are plotted relative to the corresponding mixed biangular reflectance in the specular-ray direction. The abscissa is the reflectance angle θ. Figures 3 and 7 highlight the effect of varying incident angle for surfaces of fixed roughness. On the other hand, Figs. 4, 5, and 6 display information for various fixed incidence angles (45, 60, and 75°, respectively) with surface roughness as curve parameter.

The off-specular peaks. The effect of incidence angle ψ on the distribution of reflected radiation can be conveniently examined with the aid of Fig. 3. This figure presents the mixed biangular reflectance distributions for a magnesium oxide specimen of intermediate surface roughness ($\sigma_m = 0.76\mu$). The trends in Fig.3 are typical of metals as well as of nonmetals when the surface roughness is comparable to or larger than the wavelength of the radiation ($\sigma_m/\lambda \gtrsim 1.0$). In the type of presentation employed in Fig. 3, a perfectly diffuse surface (i.e., one which obeys Lambert's cosine law of reflection) would have a constant value of the relative biangular reflectance equal to 1.0.

The results for near-normal incidence, $\psi = 10°$, approach the diffuse limit. As the angle of incidence increases, it is apparent that the corresponding

reflectance distributions differ markedly from that for a diffuse surface. For incidence at $\Psi = 45^\circ$, the distribution displays weak local maxima at the specular-reflection angle ($\theta = 45^\circ$) and at approximately $\theta = 80^\circ$. As Ψ increases still further, the maximum in the vicinity of $\theta = 80^\circ$ grows rapidly, until, at $\Psi = 75^\circ$, the off-specular maximum dominates the distribution. This off-specular peak is quite different in shape from the sharp, specular-reflection maximum occuring on a smoother surface. In Fig. 6, such a specular reflection peak is exhibited by the surface with $\sigma_m = 0.23\mu$ at $\theta = \Psi = 75^\circ$. Thus, it is evident that the diffuse distribution is approached only when the angle of incidence is near normal.

Distributions of mixed and plane-polarized reflectances. Inasmuch as the off-specular peak phenomenon is manifested at intermediate and large angles of incidence, more detailed consideration is given to the reflection distributions corresponding to incidence at such angles. Figures 4 through 7 have been prepared in this connection. The first three of these show the effect of varying surface roughness at fixed angles of incidence $\Psi = 45$, 60, and 75° for magnesium oxide. Figure 7 pertains to aluminum coated ground glass and will be discussed later.

Each of Figs. 4 to 6 displays the plane-polarized and mixed biangular reflectance distributions for four magnesium oxide specimens ($\sigma_m = 0.23$, 0.76, 1.9, and 5.8μ). The distributions of the mixed radiation are shown as blackened circles through which solid lines have been passed, and the plane-polarized components are represented by open circles connected by dashed lines. In all cases, the component (s), polarized perpendicular to the plane of incidence, lies above the solid curve. The component (p), polarized parallel to the plane of incidence, lies below the solid curve. According to equation (4), the mixed reflectance should be the average of the plane-polarized components. In point of fact, the average of the dashed curves is very nearly, but not quite, coincident with the

corresponding solid curve. This slight disparity occurs because the latter was not corrected for the polarization introduced by the spectrometer. The presentation of the uncorrected curve was purposeful in that it was desired to indicate to what extent the measurements are affected by the spectrometer-induced polarization.

The results for the smoothest surface in Figs. 4 to 6, $\sigma_m = 0.23\mu$, display a distinct peak in the mixed reflectance at the specular angle $\theta = \psi$. For a perfectly specular-reflecting surface, a peak would appear only in the vicinity of the specular angle, while at all other angles, the biangular reflectance would be zero. Furthermore, the peak would be symmetrical about $\theta = \psi$, with a base-width that depends on the solid angle of the optics. Thus, the $\sigma_m = 0.23\mu$ surface does not represent pure specular reflection, since the biangular reflectance at angular positions away from the specular region is not zero. In addition, the peak is not symmetric, showing somewhat larger reflectances in the region $\theta > \psi$. This skewing is presumably due to the off-specular peak mechanism.

An examination of each of Figs. 4 to 6 reveals that the peak at the specular-reflection angle decreases with increasing surface roughness while, at the same time, the off-specular peak emerges. For those surfaces showing a negligible specular peak, the magnitude of the off-specular peak increases with larger angles of incidence. In some cases, the intensity at the off-specular peak is 3 or 4 times the intensity in the specular-ray direction.

The plane-polarized biangular reflectance distributions in Figs. 4 to 6 provide further information about the reflection process. Considering the smoothest surface, $\sigma_m = 0.23\mu$, it is interesting to note that the contributions of the s- and p-components to the reflectance in the specular direction are in qualitative accord with the predictions of electromagnetic theory. According to the theory, the p-component of the reflected radiation is zero when an

optically smooth dielectric surface is irradiated by an unpolarized beam incident at the polarizing angle (Brewster angle). For magnesium oxide, the Brewster angle is 60.2°, which is approximately equal to the angle of incidence in Fig. 5. Correspondingly, in that case, the p-polarized component contributes very little to the specular peak. At an incidence angle $\Psi = 45°$ (Fig. 4), the p-component contributes somewhat more, and at $\Psi = 75°$ (Fig. 6), it contributes significantly, as predicted by the electromagnetic theory. For the rougher surfaces, the predictions of electromagnetic theory are not expected to apply. For such surfaces, the experimental data show that whenever there is an inflection in the reflectance distribution at the specular-ray direction, the s-component appears to be responsible.

In addition, other features of the polarized components may be noted. In Fig. 4, the p-component remains almost constant with reflection angle Θ, while the s-component gives the shape to the mixed reflectance distribution. In Figs. 5 and 6, however, both the s- and p-polarized components contribute to the off-specular peaks. This is in good agreement with models of the reflection process that postulate the presence of mirror-like surface elements. From such a model, it is expected that for the incidence angle of Fig. 4 ($\Psi = 45°$), little augmentation of p-polarized light would occur in the off-specular peak region. This is because the off-specular peak region of that figure includes angular directions corresponding to reflection at the Brewster angle from surface facets. On the other hand, for the angles of incidence corresponding to Figs. 5 and 6, the off-specular peak region does not include angular directions corresponding to Brewster-angle reflection from the facets.

The effect of incidence angle on the plane-polarized and mixed biangular reflectance distributions for aluminum coated ground glass is shown in Fig. 7. The figure pertains to a surface with roughness $\sigma_m = 2.8\mu$. The data are presented in a manner similar to that used in the foregoing figures. The feature

that is immediately observable in Fig. 7 is the accentuation of the off-specular peak with increasing angle of incidence. Both the s- and p-polarized components contribute to the off-specular peaks for all three incidence angles. This finding is consistent with the model which pictures the surface as consisting of mirror-like facets. For the aluminum coating, the Brewster angle is large ($\sim 80^\circ$). In addition, the Brewster angle for metals corresponds to the angle of incidence for a minimum (rather than zero) reflectance of p-polarized light after specular reflection. This minimum reflectance of the p-component is typically large (78 percent for aluminum). For the incidence angles $\psi = 45$ and 60°, the region of the off-specular peaks does not include angular directions corresponding to Brewster-angle reflection at the facets. In the case of the 75° incidence, Brewster-angle reflection at the facets may fall into the region of the off-specular peaks. However, owing to the aforementioned large reflectance at the Brewster angle, this does not significantly diminish the contribution of the p-component.

As a final point in connection with Fig. 7, it is apparent that the relative biangular reflectance in the normal direction ($\theta = 0^\circ$) is considerably lower than for the surfaces of similar roughness in Figs. 4 to 6. This may be made plausible by noting that for incidence at large angles on a rough surface, there would be considerable shadowing of the roughness valleys. When the reflection occurs primarily at the surface, as with a metal, this causes an apparent low reflectance in the direction of the surface normal. On the other hand, for the magnesium oxide ceramic, there is considerable internal scattering of light. Therefore, the shadowing of the roughness valleys is partially offset by the internally-reflected light which re-emerges from the surface.

The definition of the biangular reflectance requires that the solid angles of incidence and reflection be infinitesimally small. The solid angles of this experiment are indeed very small, but necessarily finite. To assess whether or

not they are small enough to permit meaningful measurements of the biangular reflectance, some data were collected using a solid angle one-fourth as large. The results are represented by the crosses in Fig. 7 for incidence at 60°. Good agreement is seen to exist between the data taken with $\Delta\omega = \pi/1024$ and $\pi/4096$.

The curves portraying the reflection distributions in Figs. 4 through 7 were terminated at various θ values less than 90°. The experimental procedure required that the entrance slit of the spectrometer be fully illuminated so that the portion of the specimen surface viewed by that instrument be confined to the interior of the illuminated spot. This necessitated the use of a wide source and narrow entrance slit widths. The maximum value of θ at which data could be taken without viewing too close to the boundary of the illuminated spot thus depended on incidence angle ψ, and the width of the source, specimen, and entrance slit. For a given incidence angle ψ, only the entrance slit width was variable. The minimum entrance slit width was determined by the minimum energy level that could be accurately sensed by the spectrometer detector.

DEGREE OF POLARIZATION

The degree of polarization of reflected light was evaluated according to either equation (5) or (7). Results for magnesium oxide are shown in Figs. 8 and 9 and for aluminum coated ground glass in Fig. 10. The abscissa is the reflection angle θ.

Figures 8 and 10a display the degree of polarization of <u>specularly</u>-reflected light for surfaces of varying roughness. The surfaces were illuminated at incidence angles ψ ranging from 10 to 87°, and the degree of polarization of the specularly reflected light ($\theta = \psi$) was determined. Such experiments naturally lend themselves to comparison with the polarization for optically smooth surfaces predicted from the Fresnel equations.

The measured results for four magnesium oxide specimens ($\sigma_m = 0.23$, 0.76, 1.9, and 5.8 μ) are represented by the solid lines in Fig. 8. The dashed line appearing in the figure represents the Fresnel equations, which were evaluated using the index of refraction of magnesium oxide.[25] The experimental curves successively approach the Fresnel prediction as the surface roughness decreases; this trend is in agreement with the work of Gorodinskii.[17] For the smoothest surface, $\sigma_m = 0.23\mu$, the peak of the curve lies at approximately the Brewster angle of 60.2°. The peaks in the other experimental curves move to larger angles θ as the surface roughness increases. In contrast, Gorodinskii's curves for ground dark glass specimens of varying roughness all peak at approximately the Brewster angle. The dark glass is characterized by strong internal absorption and weak internal scattering. The observed difference in the results is attributed to the strong, internal scattering in the magnesium oxide ceramic.

A presentation of results similar to Fig. 8, but for aluminum coated ground glass specimens, is contained in Fig. 10a. The solid lines connect data points for surfaces having roughnesses $\sigma_m = 0.33$, 0.45, 0.85, and 2.8 μ. In addition, data points for a polished surface (polished glass coated with aluminum) are shown connected by a dashed curve. This dashed curve was calculated from the Fresnel equations [26] using the index of refraction and extinction coefficient for an evaporated aluminum film at $\lambda = 0.5\mu$.[27] Excellent agreement is seen to exist between the Fresnel prediction and the experimental data. As surface roughness decreases, the curves do not tend successively toward the Fresnel curve. Instead, the surface with $\sigma_m = 0.45\mu$ shows a greater degree of polarization than that with $\sigma_m = 0.85\mu$, and the latter a greater degree of polarization than the $\sigma_m = 2.8\mu$ surface. However, the results for the $\sigma_m = 0.33\mu$ surface suggest

[25] American Institute of Physics Handbook, second edition, 1963, McGraw-Hill, New York, N.Y., p. 6-12.

[26] Handbuch der Physik, vol. 20, Springer-Verlag OHG, Berlin, 1928, p. 240.

[27] American Institute of Physics Handbook, second edition, 1963, McGraw-Hill, New York, N.Y., p. 2-107.

that a further decrease in surface roughness would lead to an approach to the Fresnel curve. The just-described behavior with decreasing surface roughness is, at present, unexplained.

It is interesting to note that all the curves in Fig. 10a peak at approximately the Brewster angle of 80°. This is in agreement with the findings of Gorodinskii. The common behavior is consistent with the fact that both the aluminum specimens of Fig. 10a and the dark glass specimens of Gorodinskii are characterized by surface reflection in the absence of internal scattering.

The variation of the degree of polarization with reflection angle θ for various fixed incidence angles ψ is shown in Figs. 9 and 10b, respectively for magnesium oxide and aluminum coated ground glass. In Fig. 9, results are given for incidence angles of 45, 60, and 75°, with surface roughness as curve parameter. Fig. 10b pertains to a surface with roughness $\sigma_m = 2.8\,\mu$, and the curve parameter is the incidence angle ψ.

The information in Figs. 9 and 10b can be conveniently discussed by again taking the work of Gorodinskii as a point of departure. For a fixed incidence angle, his degree of polarization curves for three different surface roughnesses all exhibit a maximum at the same reflection angle θ, which will be designated here as θ_{max}. Gorodinskii used fixed incidence angles ψ of 45, 60, and 70°. He presents the following experimentally-based relation between ψ and θ_{max}

$$\psi + \theta_{max} = 2\theta_B \tag{8}$$

where θ_B is the Brewster angle for dark glass. Equation (8) can also be derived from the mirror-like facet model of surface reflection.

For each of the fixed incidence angles of Fig. 9, the curves for the various surface roughnesses do not all exhibit a pronounced peak at the same reflection angle θ. Using $\theta_B = 60.2^{\circ}$ for magnesium oxide, equation (8) would predict peaks at 75.4 , 60.4 , and 45.4°, respectively for $\psi = 45$, 60 , and 75°. Clearly,

equation (8) does not describe the trends in Fig. 9. This is attributed to the effect of internal reflections.

For the aluminum coated ground glass in Fig. 10b, better agreement with equation (8) is to be expected. This is because internal scattering does not affect the reflection process for the aluminum surfaces. The data points in Fig. 10b between $\theta = 80$ and 89° for $\psi = 75$, 80, and 85° are omitted to preserve clarity. Upon applying equation (8) for $\theta_B = 80^\circ$ and recognizing that θ must be less than 90°, one obtains θ_{max} values of 90 , 90 , 85 , 80 , and 75° when $\psi = 45$, 60 , 75 , 80 , and 85°. The trends and general locations of the peaks in Fig. 10b are in agreement with the predictions from equation (8), thus further substantiating the model consisting of elementary mirror-like surface facets.

NORMAL BIANGULAR REFLECTANCE

The mixed normal biangular reflectance for incidence at angle ψ is presented in Fig. 11. Four curves for magnesium oxide and one for aluminum coated ground glass are shown. Each of the curves corresponds to a particular surface roughness σ_m. Thus, the four magnesium oxide curves serve to inter-relate the biangular reflectance distributions of Figs. 3 to 6. Similarly, the curve for aluminum coated ground glass in Fig. 11 serves to inter-relate the data in Fig. 7.

The values of the normal biangular reflectance are plotted relative to reference quantities X that are listed in the legend of Fig. 11. The reference quantity for magnesium oxide is the mixed normal biangular reflectance corresponding to 10° incidence on the $\sigma_m = 0.23\mu$ surface. The results for aluminum coated ground glass are referred to the normal biangular reflectance for 10° incidence.

Certain aspects of the results in Fig. 11 are worthy of discussion. For magnesium oxide, the curves for the two intermediate surface roughnesses lie

between the curves for the smoothest and the roughest surfaces. Also, the variation of the magnesium oxide data with ψ is much less than that of the data for aluminum coated ground glass. This is explained by the stronger shadowing effect at large incidence angles experienced by the latter. The shadowing effect for magnesium oxide is neutralized by internal scattering.

An important additional finding may be deduced by applying the results of Fig. 11. The variation of the mixed normal biangular reflectance with ψ is generally small for magnesium oxide. In particular, for the $\sigma_m = 0.76\mu$ specimen, the ordinate decreases by about 16 percent as ψ ranges from 10 to 75°. In Fig. 3, however, the mixed biangular reflectance ratios at $\theta = 0^\circ$ decrease by 86 percent for ψ in this range. Thus, the variation in the magnitude of the off-specular peak with incidence angle would be considerably amplified if Fig. 3 were to be replotted on an absolute basis. Similar remarks apply to the data shown in Figs. 4 to 7.

ACKNOWLEDGMENT

The support of the National Aeronautics and Space Administration under Grant NsG 137-61 is gratefully acknowledged.

Table 1. Grits used in preparation of specimens and resulting rms mechanical roughness σ_m

Specimen Material	Grit Diameter and Type	σ_m, Microns
Mag. Oxide	5.0μ alum. oxide	0.23
Mag. Oxide	22.5μ alum. oxide	0.76
Mag. Oxide	31μ alum. oxide	1.9
Mag. Oxide	165μ alum. oxide	5.8
Alum. Coated Ground Glass	polished	$<$ 0.004
Alum. Coated Ground Glass	3.0μ alum. oxide	0.33
Alum. Coated Ground Glass	5.0μ alum. oxide	0.45
Alum. Coated Ground Glass	22.5μ alum. oxide	0.85
Alum. Coated Ground Glass	63μ alum. oxide	2.8

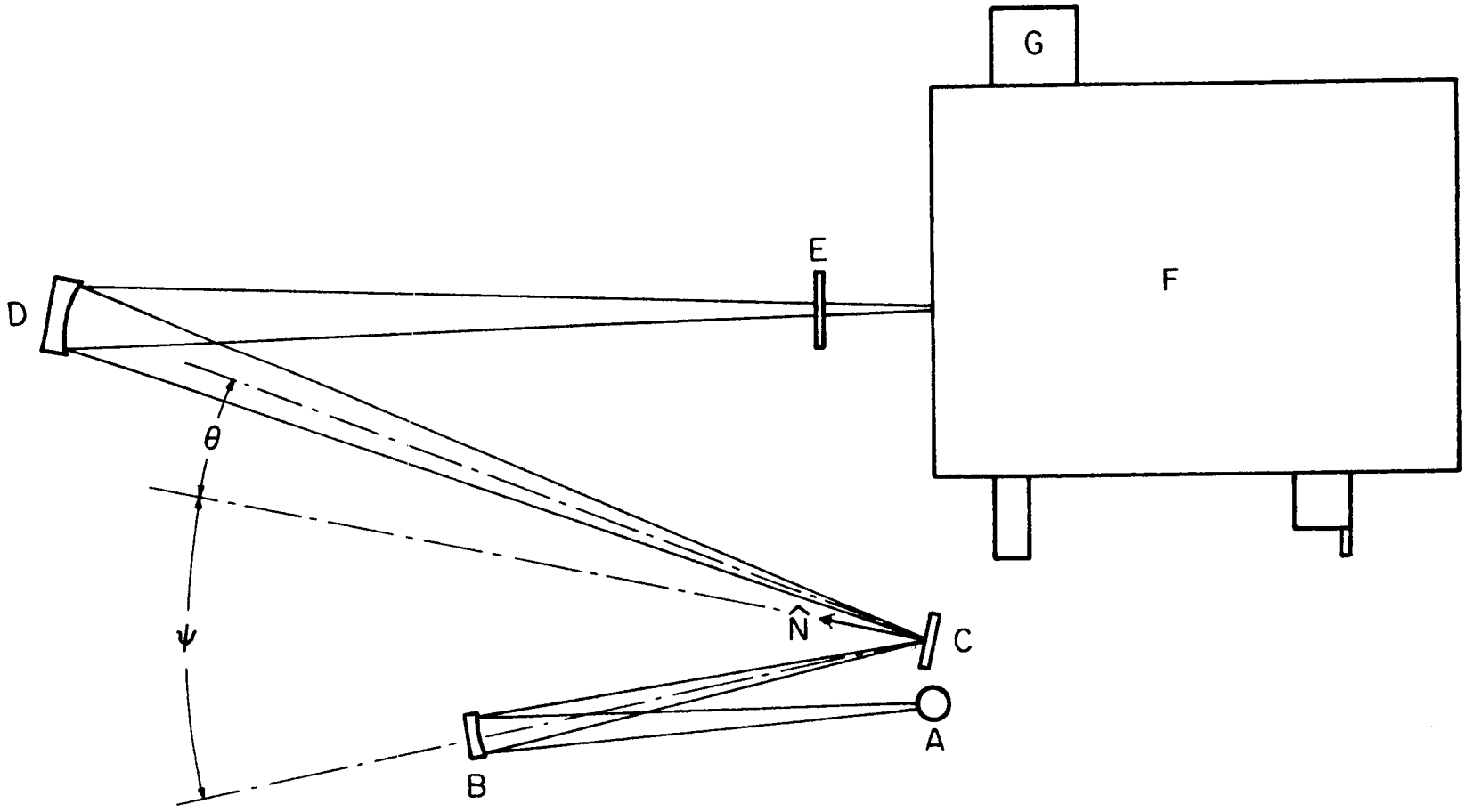

Fig. 1 Schematic diagram of experimental apparatus.

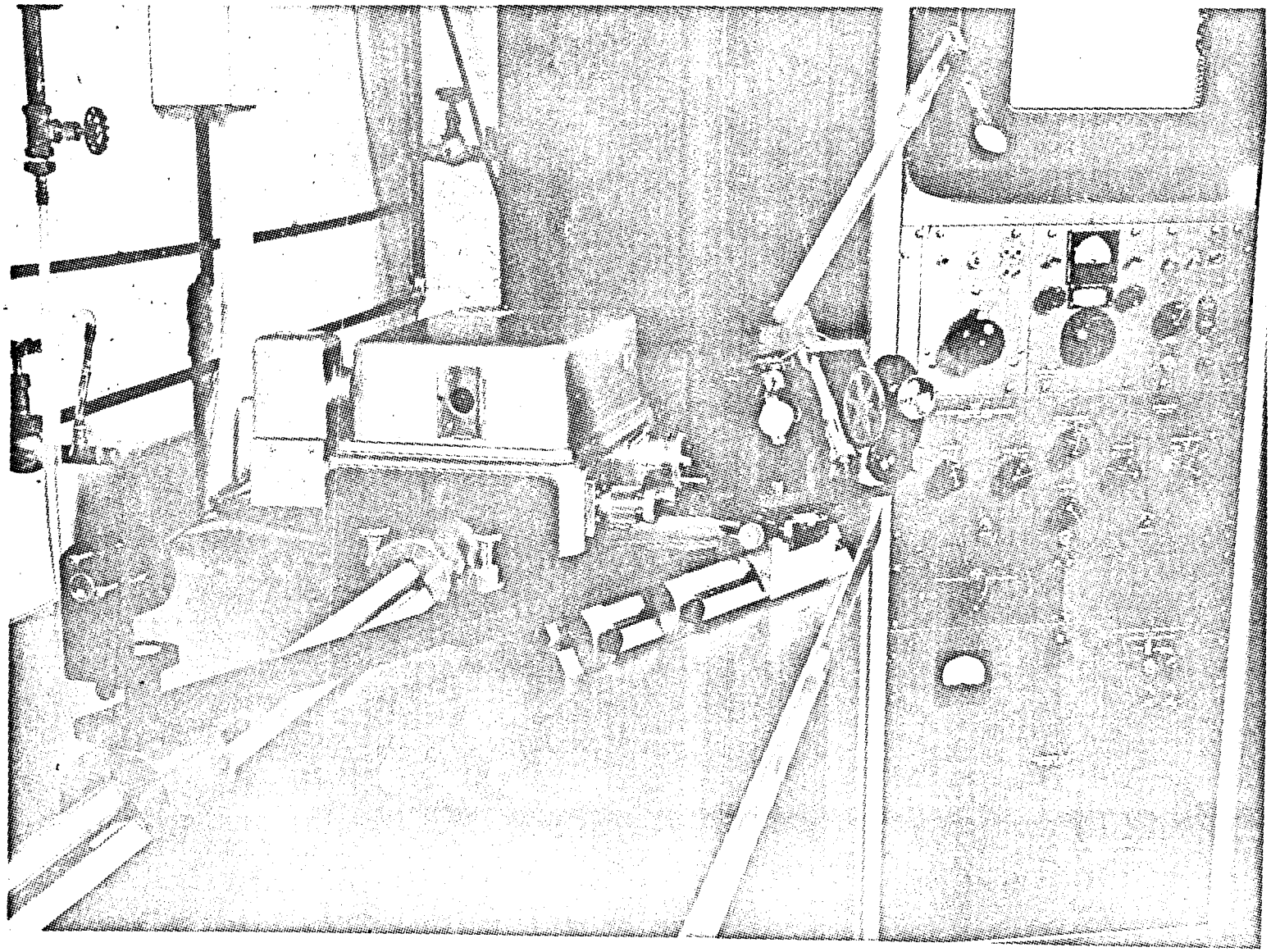

Fig. 2 View of entire test apparatus.

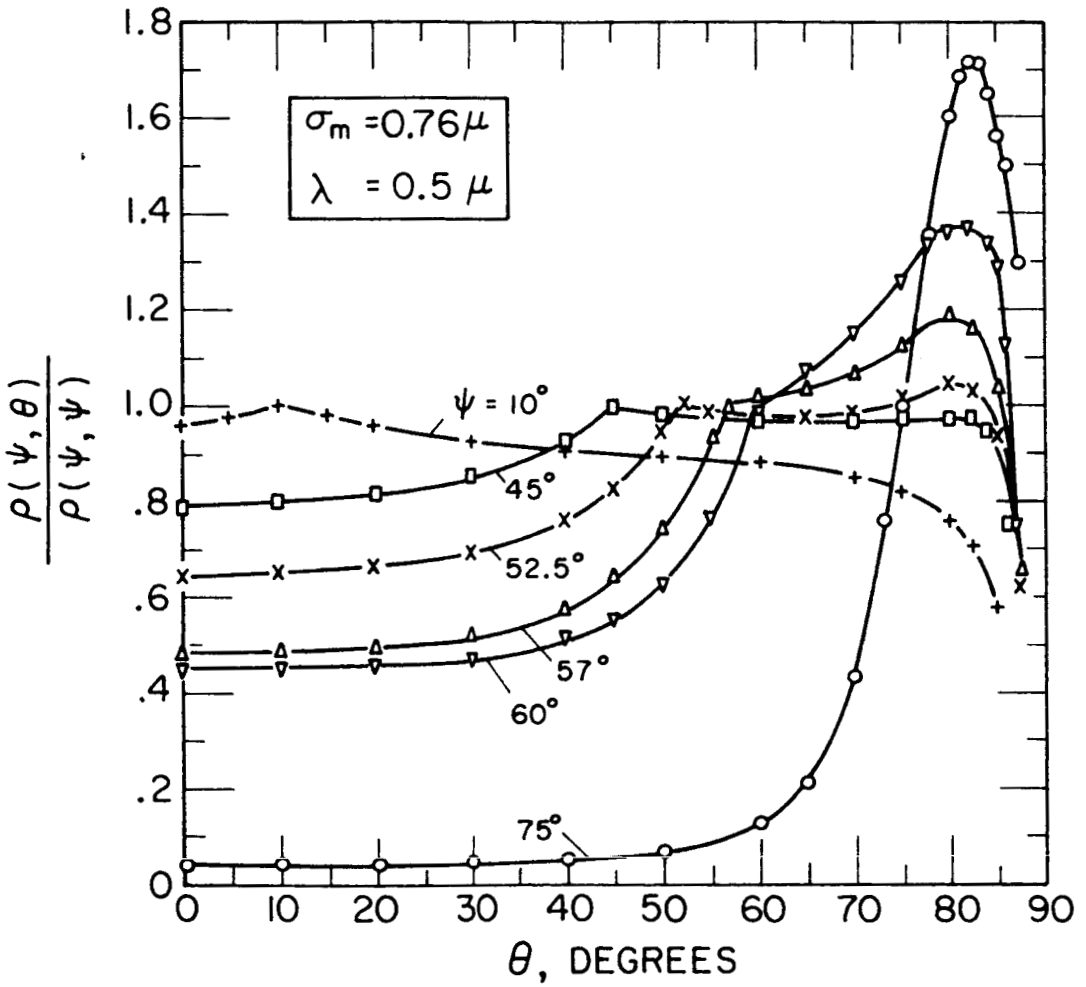

Fig. 3 Angular distribution of mixed biangular reflectance for various incidence angles Ψ, magnesium oxide ceramic.

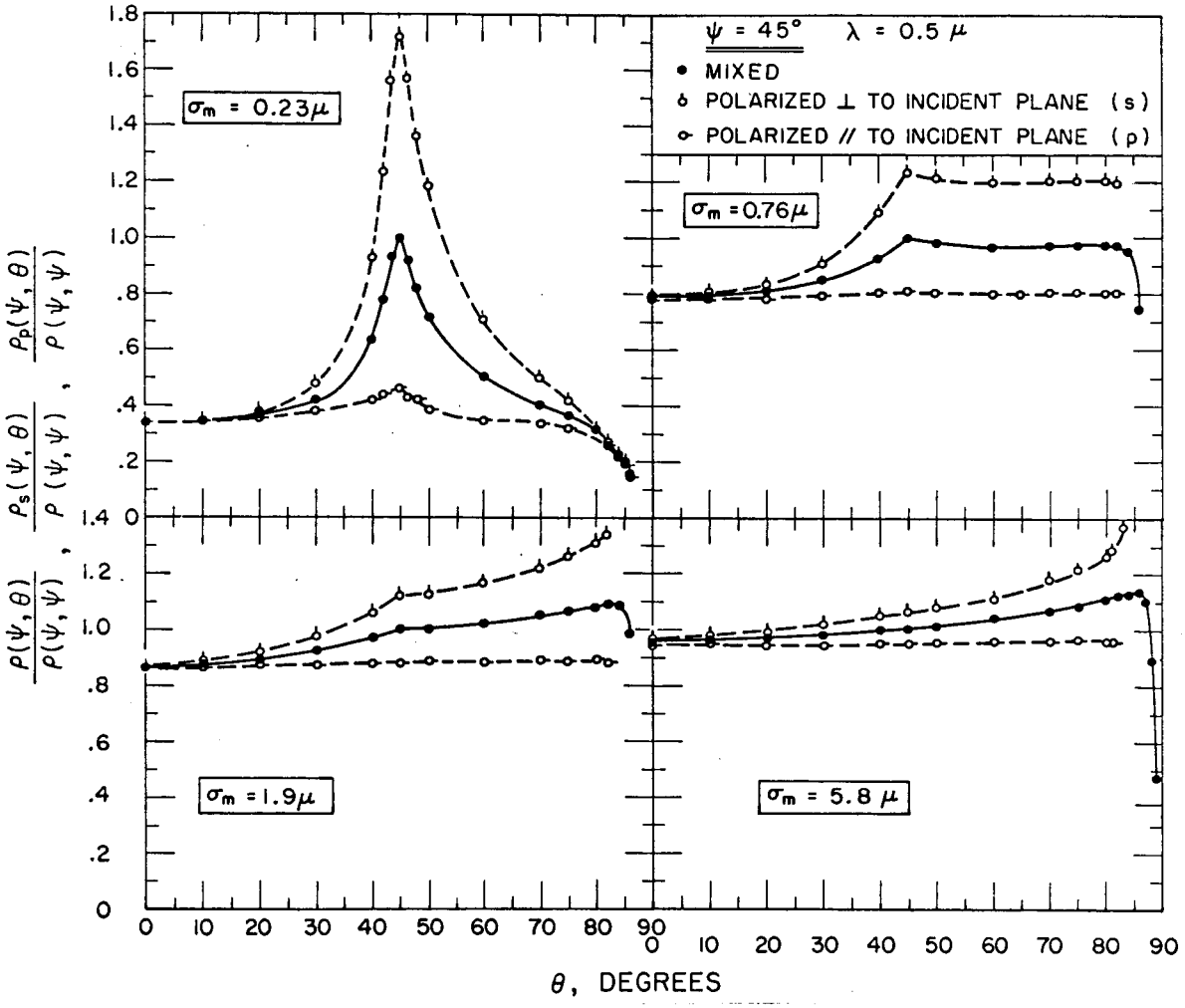

Fig. 4 Angular distributions of mixed and plane-polarized biangular reflectances, magnesium oxide ceramic. Angle of incidence $\Psi = 45^{\circ}$.

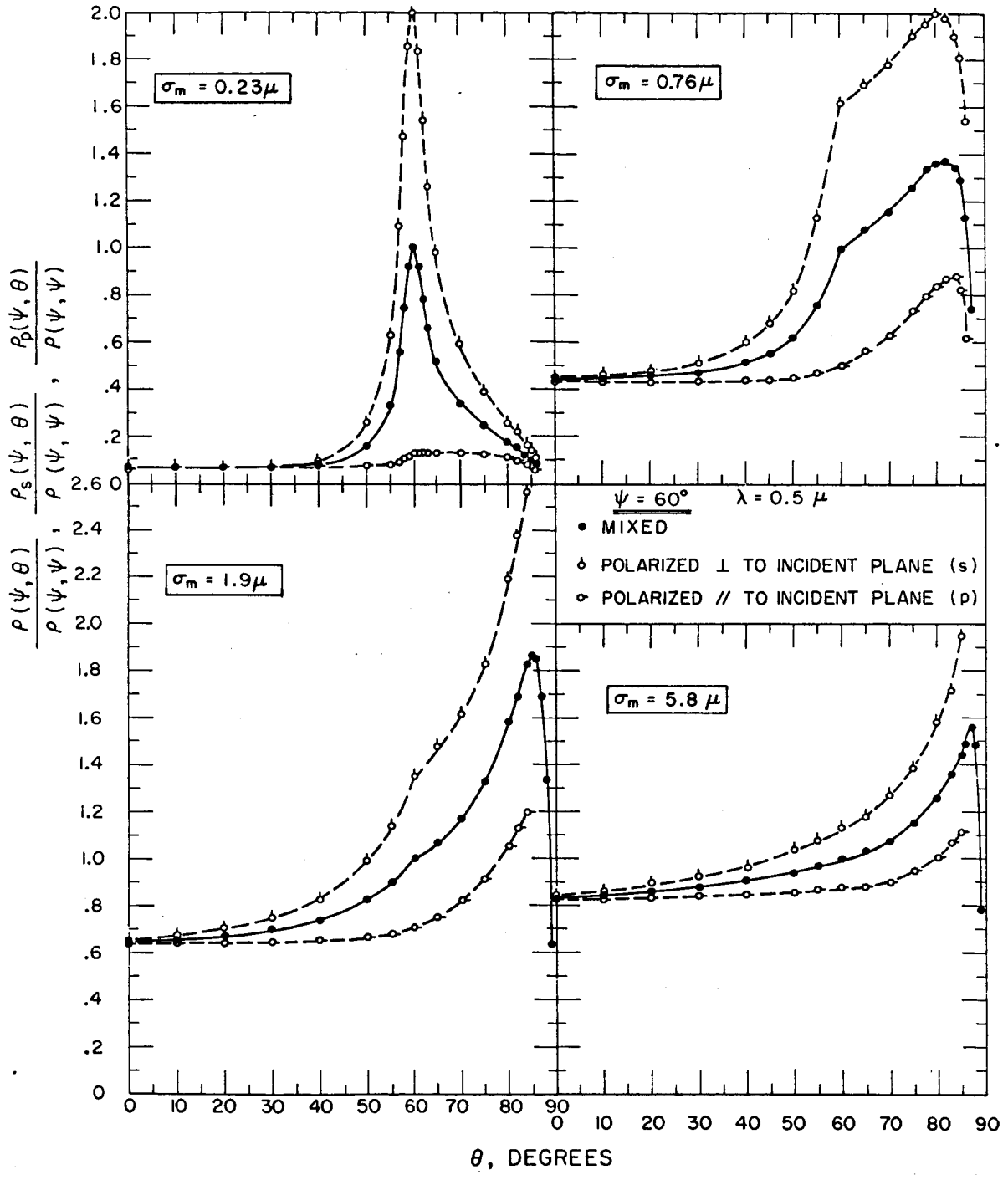

Fig. 5 Angular distributions of mixed and plane-polarized biangular reflectances, magnesium oxide ceramic. Angle of incidence $\psi = 60^{\circ}$

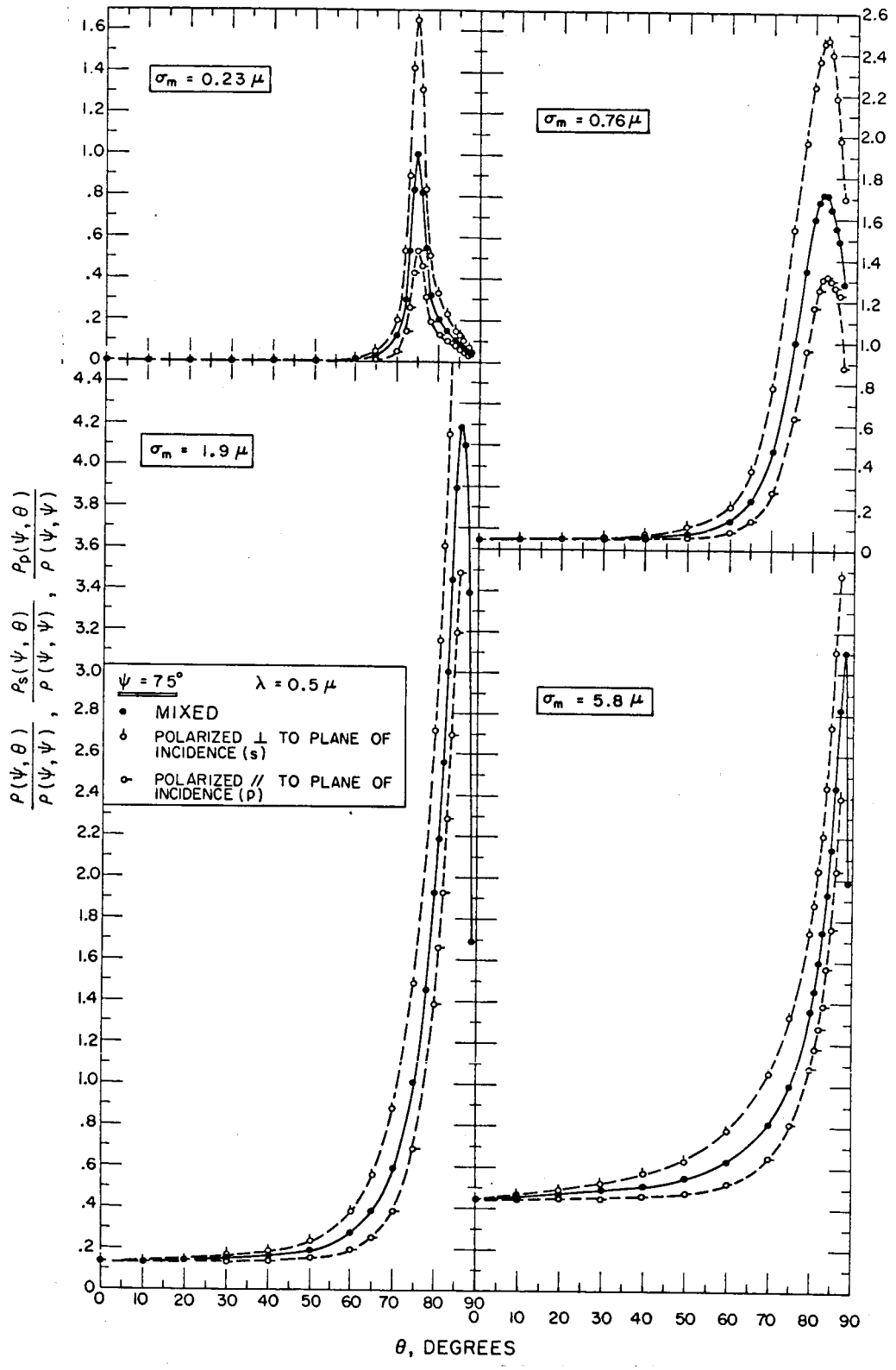

Fig. 6 Angular distributions of mixed and plane-polarized biangular reflectances, magnesium oxide ceramic. Angle of incidence $\psi = 75^{\circ}$.

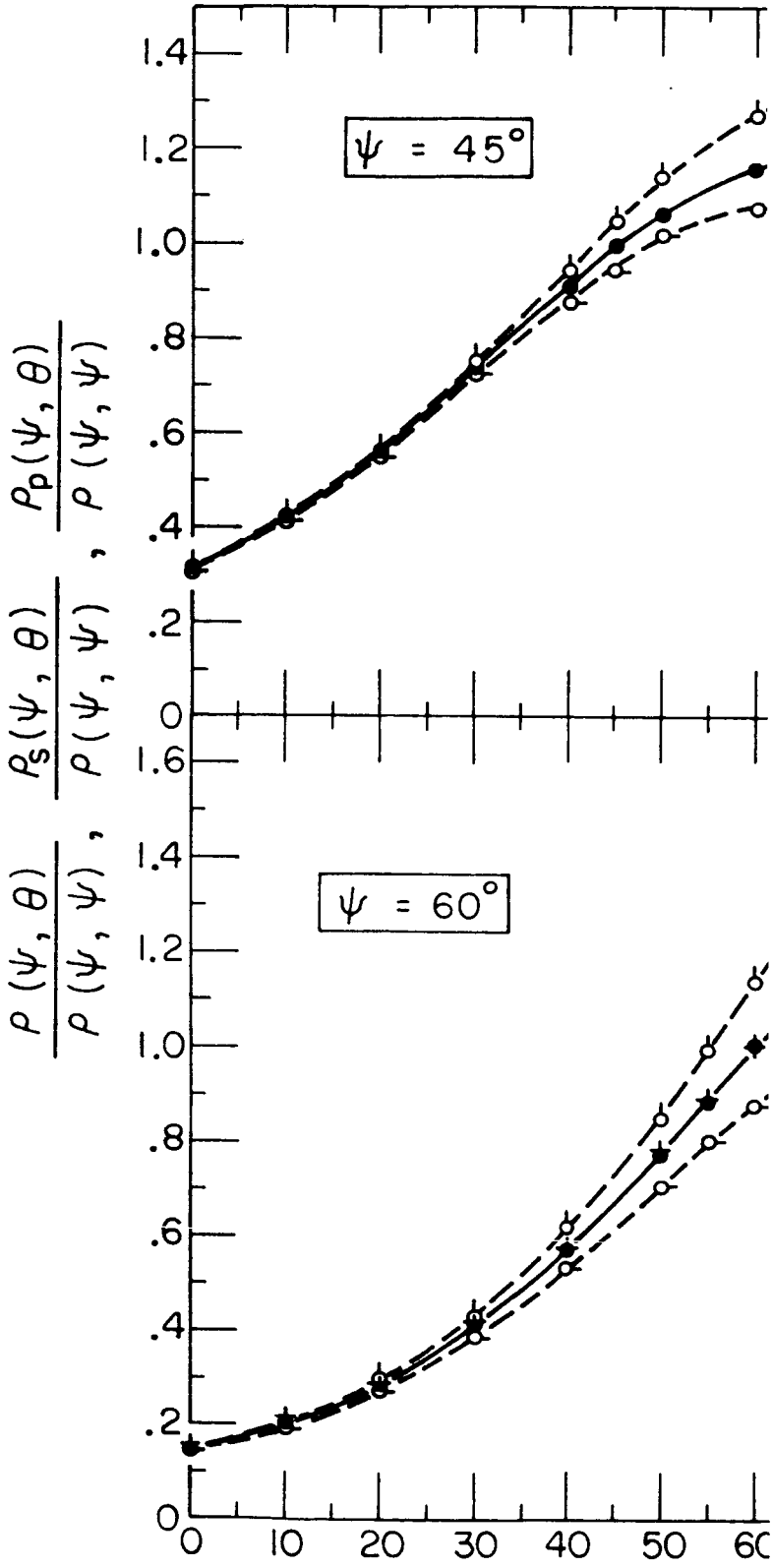

Fig. 7 Angular distributions of mixe

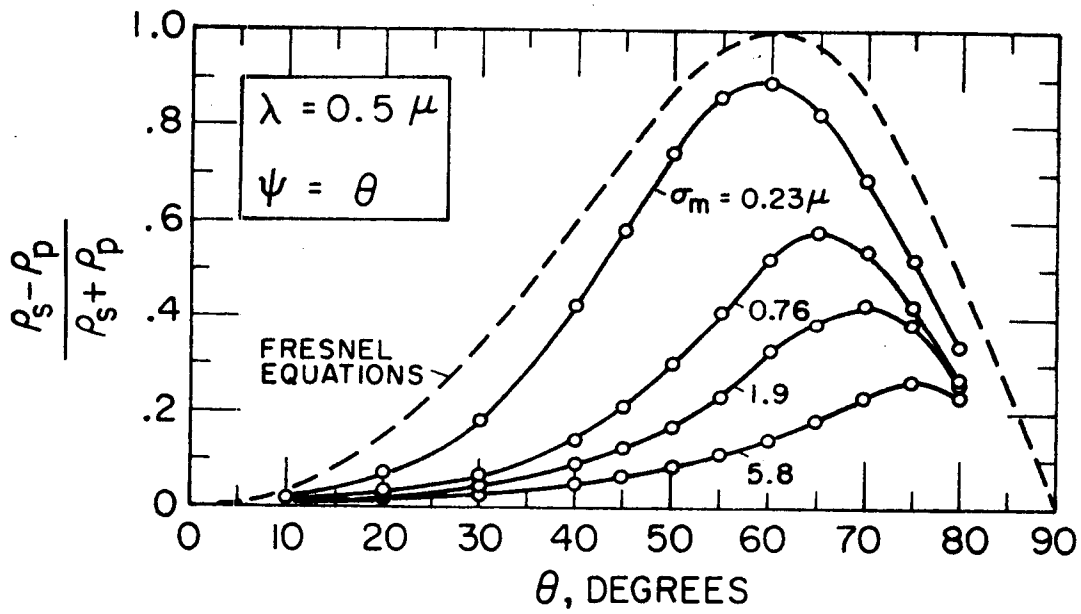

Fig. 8 Degree of polarization in the specular direction $\theta = \psi$ as a function of incidence angle ψ, magnesium oxide ceramic.

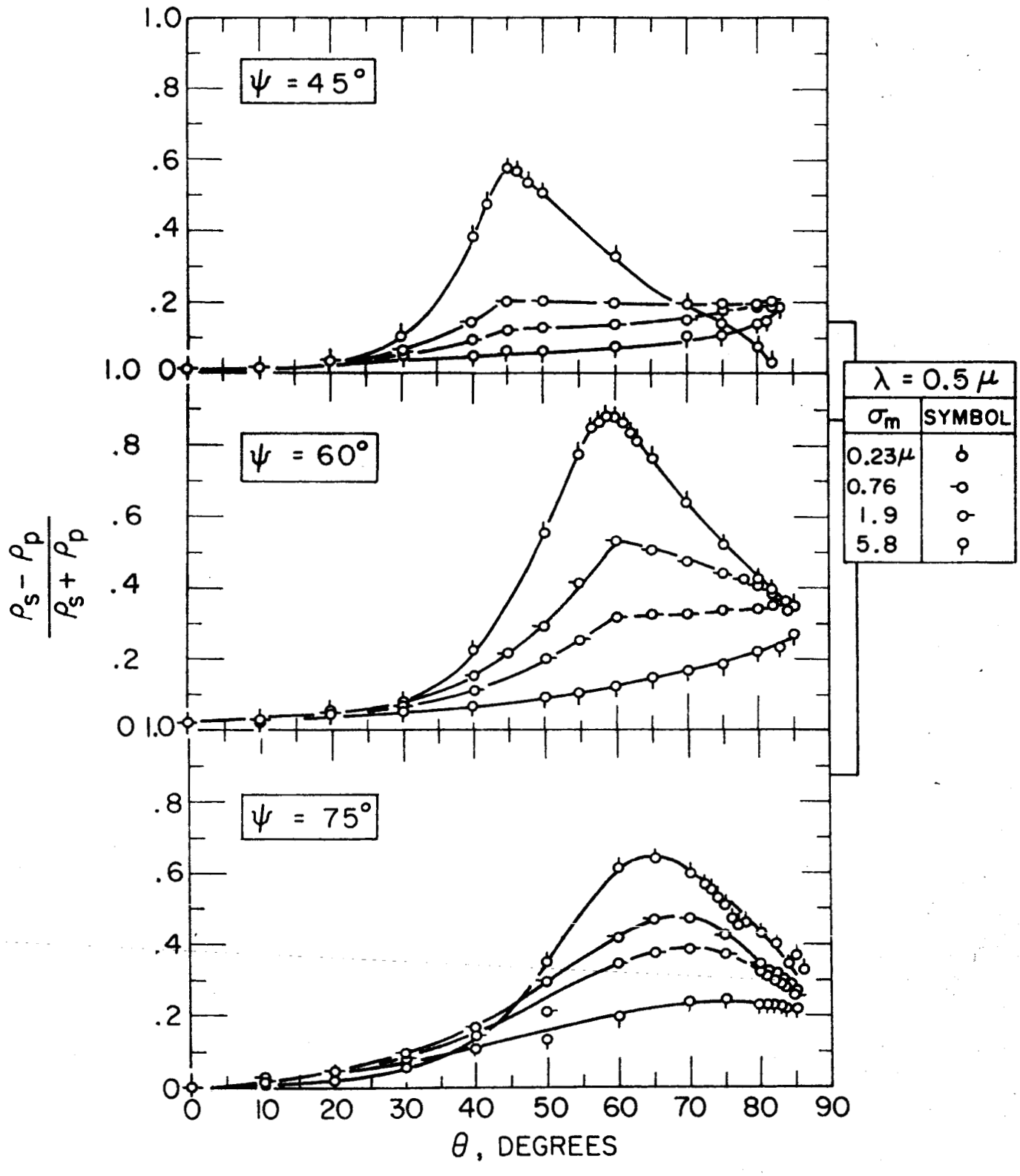

Fig. 9 Angular distributions of degree of polarization for three fixed incidence angles ψ, magnesium oxide ceramic.

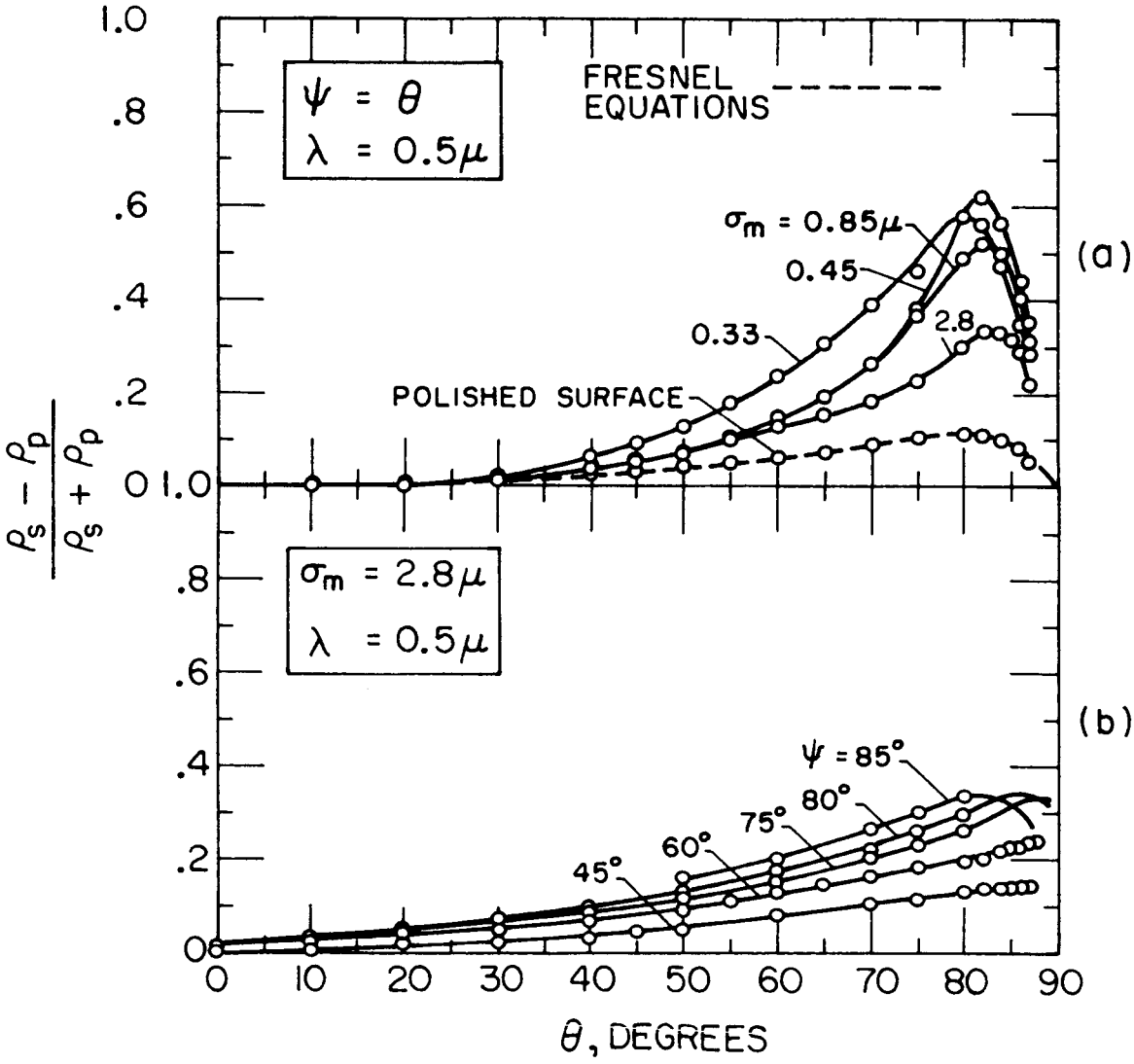

Fig. 10 Aluminum coated ground glass. (a) Degree of polarization in the specular direction $\theta = \psi$ as a function of incidence angle ψ. (b) Angular distribution of degree of polarization for several fixed incidence angles ψ.

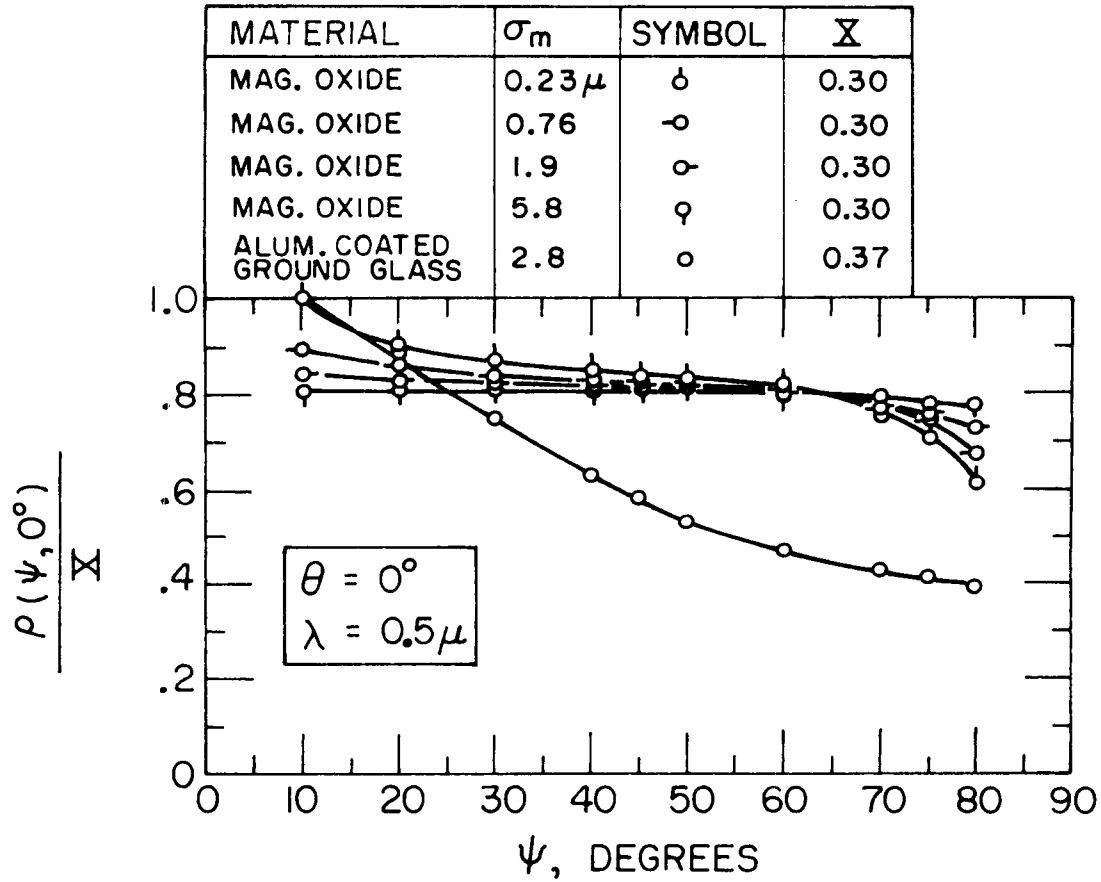

Fig. 11 Mixed biangular reflectance in direction of surface normal ($\theta = 0^{\circ}$) as a function of incidence angle Ψ.